Discovery of cryptotephra at Middle–Upper Paleolithic sites Arma Veirana and Riparo Bombrini, Italy: a new link for broader geographic correlations

Published version:

DOI:10.1002/jqs.3158

(Article begins on next page)

Discovery of cryptotephra at Middle-Upper Paleolithic sites Arma Veirana and Riparo Bombrini, Italy: A new link for broader geographic correlations

Authors:

Jayde N. Hirniak (corresponding author)[a]
Email: jhirniak@asu.edu

Eugene Smith[b]
Email: gene.smith@unlv.edu

Racheal Johnsen[b]
Email: racheal.johnsen@unlv.edu

Minghua Ren[b]
Email: minghua.ren@unlv.edu

Jamie Hodgkins[c]
Email: jamie.hodgkins@ucdenver.edu

Caley Orr[c,d]
Email: caley.orr@ucdenver.edu

Fabio Negrino[e]
Email: fabio.negrino@unige.it

Julien Riel-Salvatore[f]
Email: julien.riel-salvatore@umontreal.ca

Shelby Fitch[b]
Email: fitchshelby@gmail.com

Christopher E. Miller[g]
Email: christopher.miller@uni-tuebingen.de

Andrea Zerboni[h]
Email: andrea.zerboni@unimi.it

Guido S. Mariani[h]
Email: guido.mariani@unimi.it

Jacob A. Harris[a]
Email: jacob.a.harris@asu.edu

Claudine Gravel-Miguel[a]
Email: cgravelm@asu.edu

David Strait[i]
Email: dstrait@wustl.edu

Marco Peresani[j]
Email: marco.peresani@unife.it

Stefano Benazzi[k]
Email: stefano.benazzi@unibo.it

Curtis W. Marean[a, l]
Email: curtis.marean@asu.edu

[a] Institute of Human Origins, School of Human Evolution and Social Change, Arizona State University, P.O. Box 874101, Tempe, AZ, 85287-4101, USA
[b] Department of Geoscience, University of Nevada Las Vegas, 4505 Maryland Parkway, Las Vegas, Nevada 89154, USA
[c] Department of Anthropology, University of Colorado Denver, 1200 Larimer Street, Denver, CO 80217-3364, USA
[d] Department of Cell and Developmental Biology, University of Colorado School of Medicine, Mail Stop F435, 13001 17th Place, Aurora, Colorado 80045, USA
[e] *Dipartimento di Antichit¨, Filosofia e Storia (DAFIST), Universit¨ di Genova (Italy), Via Balbi 2, 16126 Genoa (Italy)*
[f] *D®partement d'Anthropologie Universit®de Montr®al, Pavillon Lionel-Groulx, 3150 rue Jean-Brillant, Montr®al, QC H3T 1N8 (Canada)*
[g] Institute for Archaeological Sciences and Senckenberg Centre for Human Evolution and Paleoenvironment, University of Tübingen, Rümelinstr. 23, 72070 Tübingen, Germany
[h] Dipartimento di Scienze della Terra "A. Desio", Università degli Studi di Milano, Via L. Mangiagalli 34, 20133 Milano, Italy
[i] Department of Anthropology, Washington University in St Louis, Campus Box 1114, One Brookings Drive, St Louis, MO 63130, USA
[j] Section of Prehistoric and Anthropological Science, Department of Humanities, University of Ferrara, I-44100 Ferrara, Italy
[k] Department of Cultural Heritage, University of Bologna, 48121 Ravenna, Italy
[l] African Centre for Coastal Palaeoscience, Nelson Mandela University, Port Elizabeth, Eastern Cape 6031, South Africa

Abstract

Chemical characterization of cryptotephra is critical for temporally linking archaeological sites. Here, we describe cryptotephra investigations of two Middle-Upper Paleolithic sites from northwest Italy, Arma Veirana (AV) and Riparo Bombrini (RB). Cryptotephra are present as small (<100 micron) rhyolitic glass shards at both sites, with geochemical signatures rare for volcanoes in the Mediterranean region. Two chemically distinct shard populations are present. The first (P1) from AV is a high silica rhyolite (>75 wt. %) with low FeO (<1 wt. %) and a K_2O/Na_2O >1 and the second (P2) is also a high silica rhyolite (>75 wt. %) but with high FeO (2.33-2.65 wt. %). Shards at RB (P3) are the same composition as P1 shards at AV, providing a distinct link between deposits at both sites. Geochemical characteristics suggest three possible sources for P1 and P3; eruptions from Lipari Island (53-37.7 ka) in Italy, the Acigöl volcanic field (180-20 ka) in Turkey and the Miocene Kirka-Phrigian caldera (18 Ma) in Turkey. Eruptions from Lipari Island are the most likely source for P1,3 cryptotephra. This study highlights how cryptotephra can benefit archaeology, by providing a direct link between AV and RB as well as other deposits throughout the Mediterranean.

Keywords:

Middle Paleolithic, Upper Paleolithic, radiocarbon dating, cryptotephra, reworking

1. Introduction

In the past decade, the use of cryptotephra (microscopic glass shards) has transformed the way scientists precisely date and link deposits in geology, paleoecology, and archaeology (Lowe, 2011; Lane et al., 2014; Lowe et al., 2015; Lowe et al., 2017). Cryptotephra preserves well in a variety of depositional environments (e.g., peat bogs, marine and lake sediments, ice cores) and can travel as far as 9,000 km from the source eruption (Smith et al., 2018), allowing for isochrons (precise temporal markers) to be established across large geographic areas (Lane *et al.*, 2014; Lowe *et al.*, 2015). Tephra must be sourced to a volcanic eruption whose age is known from independent dating methods to provide a precise chronological marker. However, unlike other material, cryptotephra can provide a marker horizon even without a calculated age due to the specific geochemical signatures associated with each eruption (Lowe, 2011; Lane *et al.*, 2014). The identified shards must show signs of minimal reworking to be a reliable stratigraphic and temporal marker (Lane *et al.*, 2014). If shards have been severely reworked, then the location is not indicative of primary deposition and therefore cannot be used as a reliable marker horizon. Given the potential for precise dating, tephra studies have become especially important in the field of archaeology for independently testing age models derived from other techniques (Douka *et al.*, 2014; Smith *et al.*, 2018), linking archaeological deposits (Barton *et al.*, 2014; Lowe *et al.*, 2015; Smith *et al.*, 2018), and assisting with dating sites older than the limit of radiocarbon dating (Veres *et al.*, 2017).

This contribution presents the results of cryptotephra investigations at two Middle-Upper Paleolithic sites, Arma Veirana and Riparo Bombrini, located in Liguria, Italy. The sites are 80 km apart and contain similar Middle-Upper Paleolithic archaeological assemblages; however, dating the Middle Paleolithic deposits at both sites has been difficult. At Arma Veirana, current radiocarbon dates for the Mousterian-bearing strata have so far been inconclusive, but they range from near the limit of radiocarbon dating to beyond the limits (possibly > 50 ka) (Hodgkins 2019). At Riparo Bombrini, there are radiocarbon dates near the dating limit as well as some dating inversions (Holt *et al.*, 2018). Therefore, for this study, we sampled the two sites in the hope of finding shards of similar composition. This would allow us to better date the assemblages, if the shards could be correlated to a radiometrically dated eruption. Additionally, it can assist in correlating the occupational history of both sites as well as establish an isochron(s) applicable to other Paleolithic sites in southern Europe. Here, we report shard compositions and suggest a stratigraphic location of the isochron at both sites based on a shard count profile and micromorphological analyses. These analyses are important to understand the depositional processes that may have affected the shards and identify a reliable isochron. These results highlight the benefits of cryptotephra correlations as well as important factors that must be considered when using this tool on archaeological sites.

2. Site Description

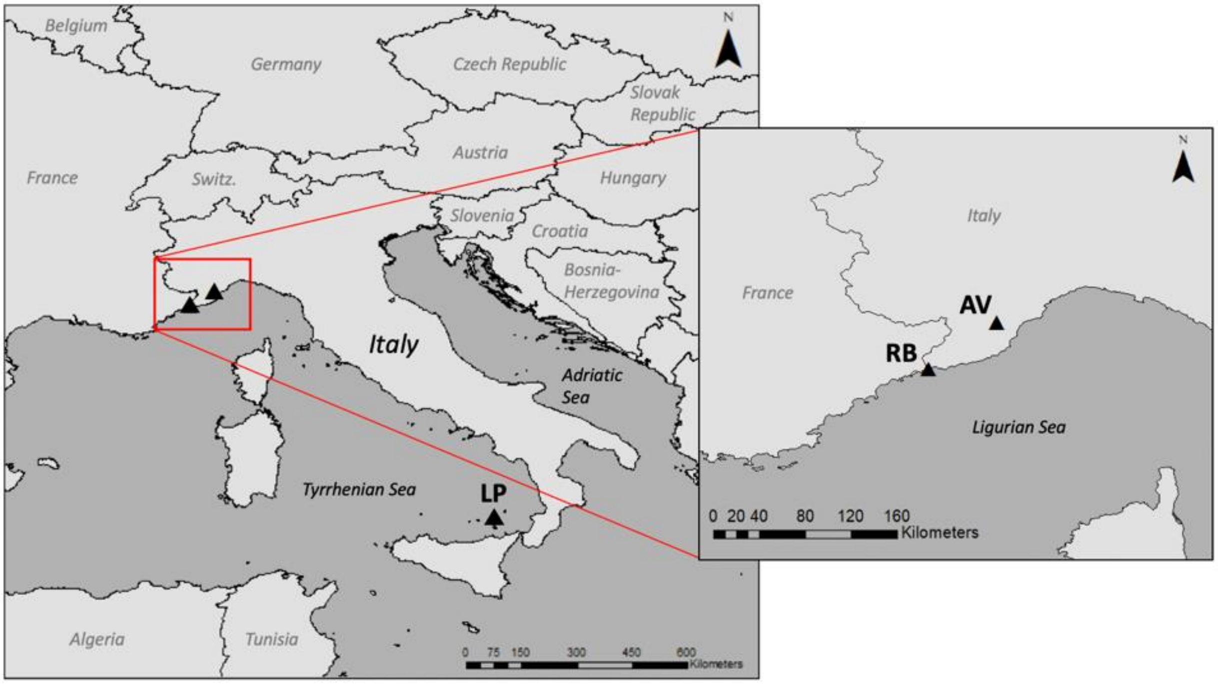

Figure 1. Location of study sites. AV is Arma Veirana located in the Ligurian pre-Alps. RB is Riparo Bombrini located at the Franco-Italian border, along the present-day coastline. LP is Lipari Island and is the location of a potential source volcano.

2.1 Arma Veirana

Arma Veirana is a limestone cave situated on the south side of Neva Valley in Liguria (44° 08' 45.4" N, 08° 04' 18.8" E) approximately 14 km from the Mediterranean coast (Fig 1). It formed through differential erosion along a fault and is carved into a north-facing cliff. Formal excavations at Arma Veirana began in 2015. The cave floor slopes upward to the south, exposing younger sediments in the back and older sediments near the mouth of the cave. *In situ* Middle and Upper Paleolithic deposits have been excavated in trenches located near the mouth of the site, suggesting that most of the deposits are undisturbed. Micromorphological analyses show that bioturbation is present at Arma Veirana; however, the amount of reworking between distinct stratigraphic units is minimal and limited to a few centimeters at the contacts. This is important to understand when identifying the exact stratigraphic location of shards (see section 5.7 for a detailed discussion).

The stratigraphic units uncovered in the main trenches are, from bottom to top, Black Mousterian (BM), Granular (Gr), Compact Strong Brown (CSB), and Rocky Brown (RB). The CSB, Gr, and BM have yielded Mousterian lithics. Each stratigraphic unit contains a mixture of material and is likely to have accumulated by colluviation and roof-fall. The BM fine fraction consists of sandy, clayey silt with sub-rounded, gravel-sized fragments of bedrock. It is dark grayish brown in color (10YR 3/2) which is clearly derived from the abundance of anthropogenic components (charcoal, bone fragments, burnt bone) (Fig 2). The Gr is dominated by a medium sandy silt that contains granules and gravel throughout. It contains a granular microstructure and is less compact than the BM. Packing voids are present, but anthropogenic components are rare (Fig 2). The proportion of comminuted charcoal and other combustion residues decrease noticeably as one moves upward in the section, which suggests less anthropogenic influence.

Radiocarbon dating of the Mousterian-bearing deposits at Arma Veirana has been unsuccessful. Oxford University and Eidgenössische Technische Hochschule (ETH) Zürich analyzed charcoal and bone samples collected on site. Analyses at ETH Zürich dated the BM to 43,781-43,121 cal a BP and the Gr to 41,721- 41,174 cal a BP. Calibration for samples were performed using OxCal 4.2 (Bronk Ramsey, 2013) and the IntCal13 calibration dataset (Reimer et al., 2013). Samples were analyzed again at Oxford University and resulted in infinite ages (> 45,000 14C a BP) except one charcoal sample in stratigraphic unit Gr (49,400 ± 1,900 14C a BP)

(Hodgkins 2019). Therefore, the exact time period of the Middle Paleolithic occupation at Arma Veirana remains inconclusive.

2.2 Riparo Bombrini

Riparo Bombrini is a collapsed rock shelter located on the Mediterranean coast near the Franco-Italian border (43° 46′ 59.6″ N, 07° 32′ 7.6″ E) (Fig 1). The site was discovered in 1887 by E. Rivière (Rivière, 1887) after railroad construction along the coast cut through the cliff, damaging and destroying a large part of the site. The remaining part of the site has been excavated in stages over the last 40 years, first in 1976 by Giuseppe Vicino (Vicino, 1984), second in 2002-2005 by Brigitte Holt (Holt *et al.*, 2018), and currently (2015-2018) by Julien Riel-Salvatore and Fabio Negrino (Riel-Salvatore and Negrino, 2018). From bottom to top, the lower Mousterian stratigraphic units are labeled as M1-M7, the upper Mousterian units as MS1-MS2, and the Protoaurignacian units as A1-A3. These excavations revealed Late Mousterian deposits and bladelet-rich Protoaurignician layers that appear undisturbed. The lithics found in the Mousterian layers have some similarities with the lithics found in CSB, Gr, and BM stratigraphic units at Arma Veirana. A modern human deciduous tooth was recovered in the Protoaurignacian deposits (Level A2) making it one of the few Protoaurignacian sites associated with diagnostic human remains (Benazzi *et al.*, 2015).

Micromorphological analyses show that instances of bioturbation appear to be more significant in the upper layers (MS1-M3) and are rare to nonexistent in the lower layers (M4-M7) (Fig 2). Anthropogenic components like charcoal, bone fragments, or burnt bone are absent at Riparo Bombrini; however, flint is present in stratigraphic units M4-M6. Because flint is not naturally occurring in the rock shelter and is likely indicative of stone tool production, this suggests there is more anthropogenic influence in these layers. Mineral constituents in each stratigraphic unit also contain variable amounts of aeolian and volcanic materials. Volcanic material is more common in the upper layers (MS1-M3) and some have been identified as highly altered porphyritic andesite. This material belongs to sediments outside of the rock shelter and are also not naturally occurring within the shelter, suggesting input through aeolian processes (see section 5.7 for a detailed discussion).

Charcoal samples from exposed hearths were collected at Riparo Bombrini in 2002-05 (Holt et al., 2018). Analyses were completed at Beta Analytic, Inc. and calibrated using OxCal 4.2 (Bronk Ramsey, 2013) and the IntCal13 calibration dataset (Reimer et al., 2013). Samples yielded eight AMS radiocarbon dates (Holt *et al.*, 2018); however, three samples (RB 47, 69, 265) produced ages that were too young and do not agree with cultural or geological context, which may be due to disturbances associated with the 19th century railroad construction (Holt *et al.*, 2018). When considering only non-problematic dates, the occupation of Riparo Bombrini is dated to 44,000 cal BP to 36,000 cal BP (see section 6.2 a detailed discussion).

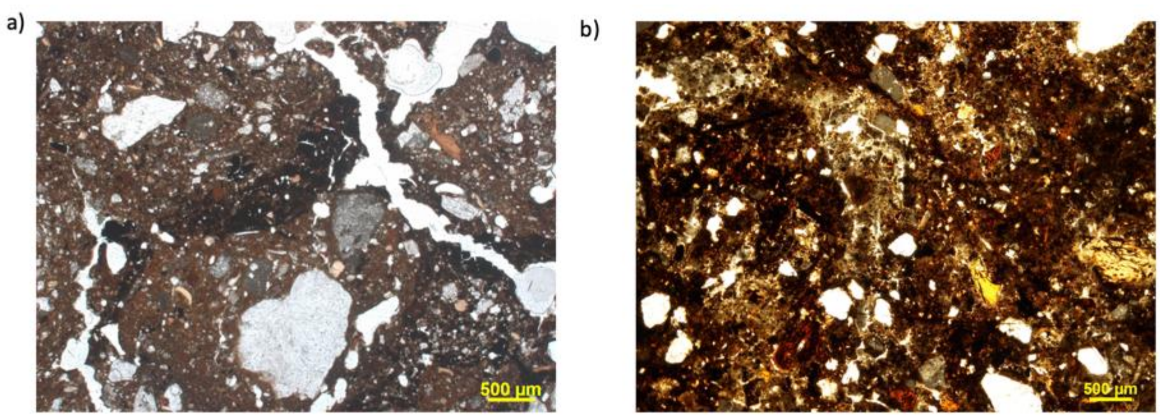

Fig 2. Photomicrographs from stratigraphic units in which cryptotephra shards were found at Arma Veirana and Riparo Bombrini. Both photos are taken in plane polarized light (PPL). **a)**, Photo of contact between BM and Gr stratigraphic units at Arma Veirana. The dark organic

lens (BM) shows mixing in the brown sediment (Gr), demonstrating that there is slight reworking between stratigraphic units. **b)**, Photo of stratigraphic unit M4 at Riparo Bombrini. Reworking is present as bioturbation forming the light-colored areas but is minimal.

3. Methods

3.1 Cryptotephra sampling and extraction

In 2017 and 2018, we sampled for cryptotephra along exposed stratigraphic sections at Arma Veirana and Riparo Bombrini, following the methods of Lane et al. (2014). At both sites, we cleaned the sections and collected 10-20 g sediment samples from the bottom-up in 2 cm intervals, creating continuously sampled columns. Each stratigraphic unit was sampled, resulting in approximately 1.5 m of sample columns at Arma Veirana (Fig 4) and 1 m at Riparo Bombrini (Fig 6).

Samples were processed at the Cryptotephra Laboratory for Archaeological and Geological Research (CLAGR) at the University of Nevada, Las Vegas (UNLV) using techniques published in Blockley et al. (2005). Due to the extremely low abundance of cryptotephra in our samples (3 shards/gram), we modified the methods following procedures successfully employed in Smith et al. (2018). Samples were air-dried, weighed, and placed in 10 mL of 10% HCL to remove any carbonates. The material was then rinsed with distilled water and wet-sieved into a 20-80 μm grain size fraction. Lithium metatungstate (LMT) heavy liquid at densities of 2.2 g/cm^3 and 2.5 g/cm^3 was used to separate the vitric component from minerals such as quartz and feldspar. LMT was added to each sample and centrifuged twice for 15 minutes at 2500 rpm to expedite the separation process. The separate was further cleaned with distilled water and then mounted on a one-inch diameter epoxy round. Rounds sat for 24 hours before being hand polished with four different clothes (6, 3, 1, and 0.25 μm). Samples were then scanned using a petrographic microscope to identify isotropic grains (potential glass shards).

Major element compositions of individual tephra grains were determined using a JEOL JSX8900 SuperProbe EPMA, equipped with four wavelength dispersive spectrometers (WDS), at the Electron Microanalysis and Imaging Laboratory at UNLV, following methodologies published in Smith et al. (2018). We used a 15kV accelerating voltage, 10nA beam current and beam size of 10 μm for operating conditions of the EPMA. We set peak and background counting times to 30 and 10 s for all elements except Na (Na was set to 10 and 5 s). To prevent element migration from beam damage, elements Na and K were counted on the first WDS cycle. The rhyolite glass standard ATHO-G, a part of the MPI-DING international standard set, was analyzed alongside glass shards on the electron microprobe to monitor instrument accuracy and precision (Jochum *et al.*, 2006). Analytical error was minimal for most elements (< ±0.2 wt. %) except for SiO_2 (±0.83 wt. %), Al_2O_3 (±0.25 wt. %), and Na_2O (±0.57 wt. %).

Conducting trace element analyses is critical to correlating tephra to its proper source. Since tephra from the same region can produce volcanic rocks with similar major elements signatures (Vinkler *et al.*, 2007; Lowe, 2011), trace elements are needed to properly identify the source. Therefore, we performed trace element analyses on the glass shards that had been analyzed for major elements. Analyses were completed at Michigan State University using a Thermo Scientific ICAP Q Quadrupole Inductively Coupled Plasma Mass Spectrometer (ICP-MS) integrated with a Photon Machines Analyte G2 193 nm excimer laser ablation system. This laser ablation system is equipped with a 15 x 15 cm HelEx sample cell for solid sample microanalyses. For our samples, we used a laser fluence of 4.1 J/cm^2 at a repetition rate of 10 Hz (10 laser hits per second). We adjusted beam diameters based on sample size and calibrated concentrations at a 110 μm pit diameter on surface scans of NIST 612, USGS basalt glass standards, and rock powder standards from the Geological Survey of Japan and the U.S. Geological Survey. The ICP-MS was tuned using surface scans of NIST 612 and the oxide production rate was kept at (ThO/Th) < 0.7% and double charged cations was ($^{137}Ba^{++}/^{137}Ba$) < 3% while performing surface scans. We subtracted backgrounds from each analysis and collected gas blanks after each standard and sample.

3.2 Statistical analyses

Statistical analyses were completed on cryptotephra compositional data using OpenBUGS, a Bayesian statistics software that uses Markov chain Monte Carlo (MCMC), following modified statistical methods from Smith et al. (2019) and Harris et al. (2017). Before running the model, all major oxide data were normalized to ensure that the comparisons between reference data were consistent. Reference data were chosen from published materials and includes a variety of compositions from both proximal and distal sources (Table S2). To reduce the impact of our biases on the results, we included potential volcano sources dated well beyond the expected age range of the layers with cryptotephra (e.g., Miocene). We calculated the standard deviation of each element within sources and between sources to determine which elements varied the most. The elements exhibiting the highest variation were included in the Bayesian model. A total of 10 major elements and 32 trace elements from 1379 samples were included in the model. We divided the compiled data into ‘training’ and ‘validation’ subsets allowing for the model performance to be tested through an out-of-sample cross validation. Model performance results for major elements show a predictability accuracy of **XX%** and results for trace elements show a predictability accuracy of **XX%**. **XX** samples were misidentified and incorrectly identified as **XX**. After model performance was assessed, the subsets of data were combined and used to predict the Arma Veirana and Riparo Bombrini archaeological samples. For the major element data, 17 samples were from Arma Veirana and three samples were from Riparo Bombrini. For the trace element data, five samples were from Arma Veirana and six samples were from Riparo Bombrini.

4. Results

4.1 Arma Veirana and Riparo Bombrini cryptotephra horizons

There are two cryptotephra populations present at Arma Veirana (population one and population two) and one cryptotephra population at Riparo Bombrini (population three). At both sites, the shards are high-silica rhyolites and are in extremely low abundance (1-8 shards/gram). Geochemical results are shown in Table 1 and Table 2. Population one (P1) has a rhyolitic composition characterized by 75.09-78.32 wt.% SiO_2, 11.6-13.47 wt.% Al_2O_3, 0.44-0.91 wt.% FeO, and a K_2O/Na_2O >1. Population two (P2) also has a rhyolitic composition with concentrations of 75.78-76.82 wt.% SiO_2, 11.27-12.27 wt.% Al_2O_3, and 2.33-2.65 wt.% FeO. Population three (P3) has concentrations of 76.64 – 76.96 wt.% SiO_2, 11.79-12.44 wt.% Al_2O_3, 0.7-0.89 wt.% FeO, and a K_2O/Na_2O >1. Trace element analyses for P1 and P3 show depletions in Ba and Sr, an Eu anomaly and an enrichment in heavy rare earth elements (HREE) (Fig 8). For P2, trace element analyses show a depletion in Sr and an enrichment in light rare earth elements (LREE) (Fig 8).

At Arma Veirana, P1 was found in stratigraphic units BM and Gr and is the most common shard composition. Shards are small (<100 μm) and appear to be rounded when viewed in epoxy mounts, but several show angular and cuspate margins. The shards are entirely glass, lack phenocrysts and several contain small vesicles (Fig 3). A shard count profile of P1 shows a few distinct peaks concentrated in the BM (Fig 5). Sample AV651 shows the highest peak and was collected at the base of the exposed stratigraphic section. It is possible that more shards are present below the collected column, but the section has not been excavated below this point. P2 is located in stratigraphic unit Gr in sample AV665. These shards are larger than population one (P1) (>100 μm) and are tabular with sharp angular corners (Fig 3). P2 did not have enough shards to generate a count profile (<3 shards).

At Riparo Bombrini, P3 was found in stratigraphic units M1 to M4 in extremely low abundance (3 shards/gram) (Fig 6). Shards are small (~80 μm) and well-rounded (Fig 3). A shard count profile of P3 shows distinct peak concentrated in M4/M3 (Fig 6).

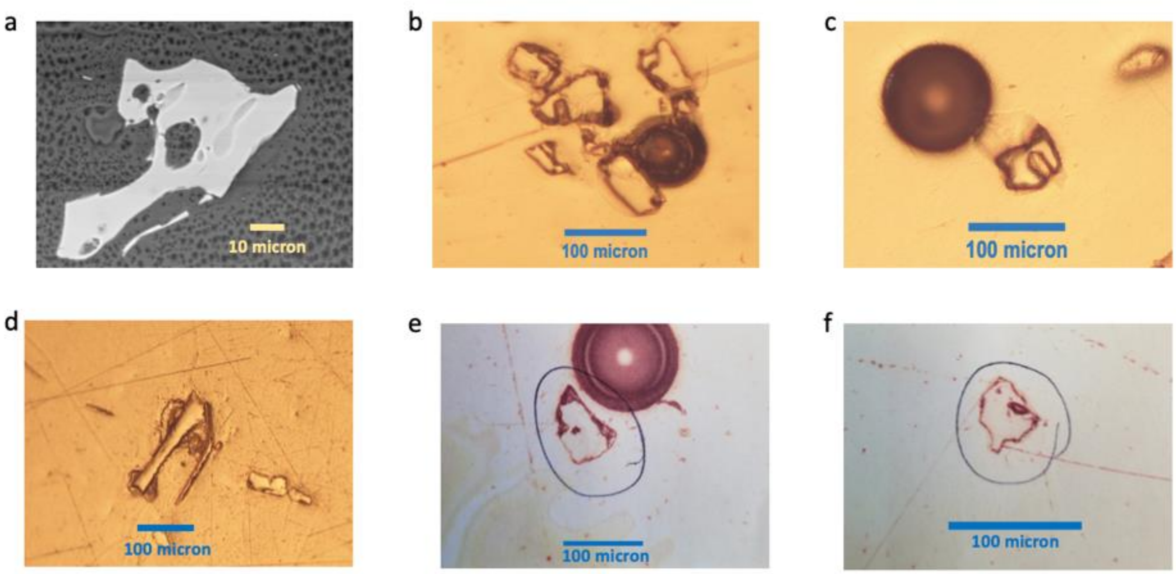

Figure 3. Examples of cryptotephra from Arma Veirana and Riparo Bombrini. Images were taken from polished epoxy rounds using plane-polarized light. Image a was taken using SEM back-scattered electrons. **a,** Shard from sample AV662 (P1). This is a high-resolution

backscattered electron image. **b,** Shards from sample AV651 (P1). **c,** Shard from sample AV655 (P1). **d,** Shard from sample AV665 (P2). **e, f,** Shards from sample RB15a (P3).

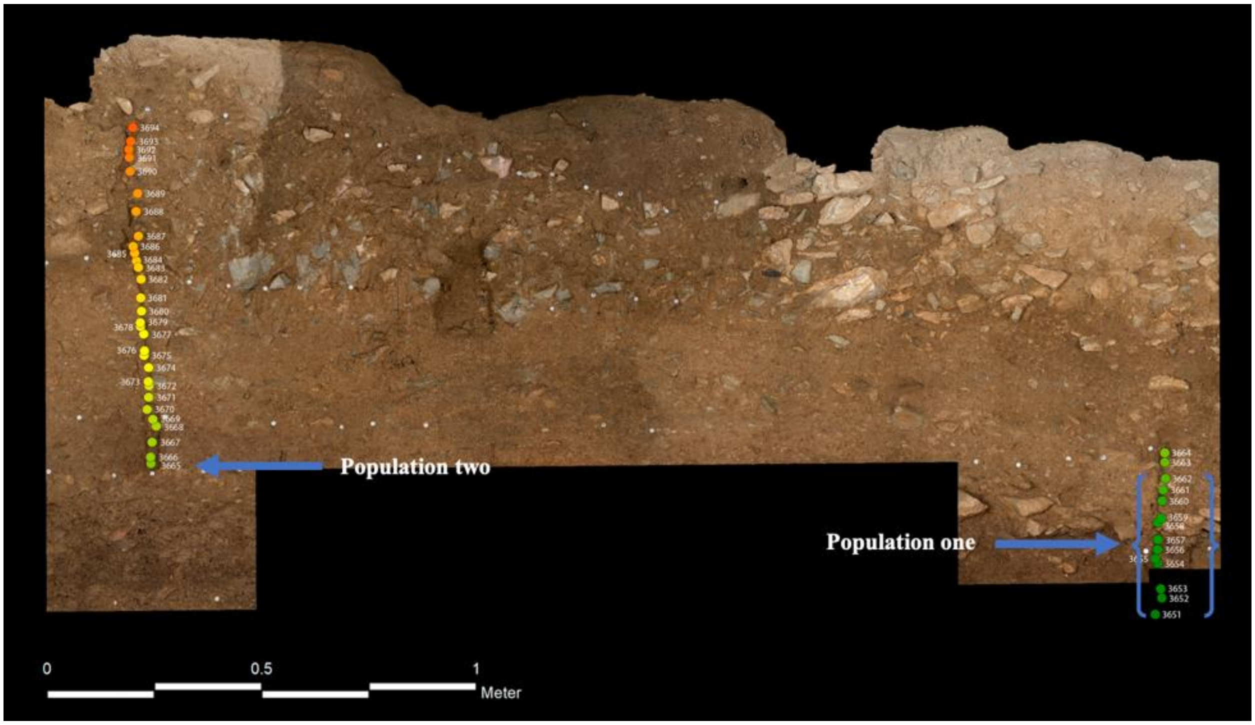

Figure 4. Location of cryptotephra sample columns at Arma Veirana. Samples were collected every 2 cm creating two continuous columns. The two columns overlap vertically by approximately 10 cm. P1 is distributed over stratigraphic units Gr and BM.

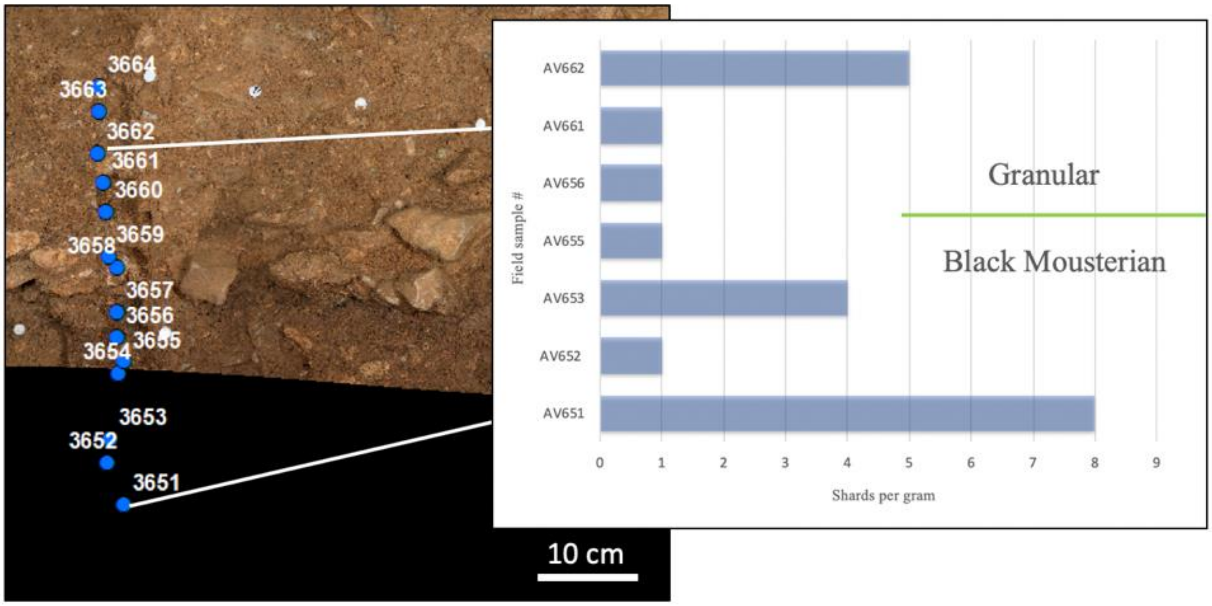

Figure 5. Shard concentrations at Arma Veirana. Samples AV651 to AV662 contain P1 shards. Numbers in the photo are field sample numbers. The y-axis represents each sample number and the x-axis shows shards per gram.

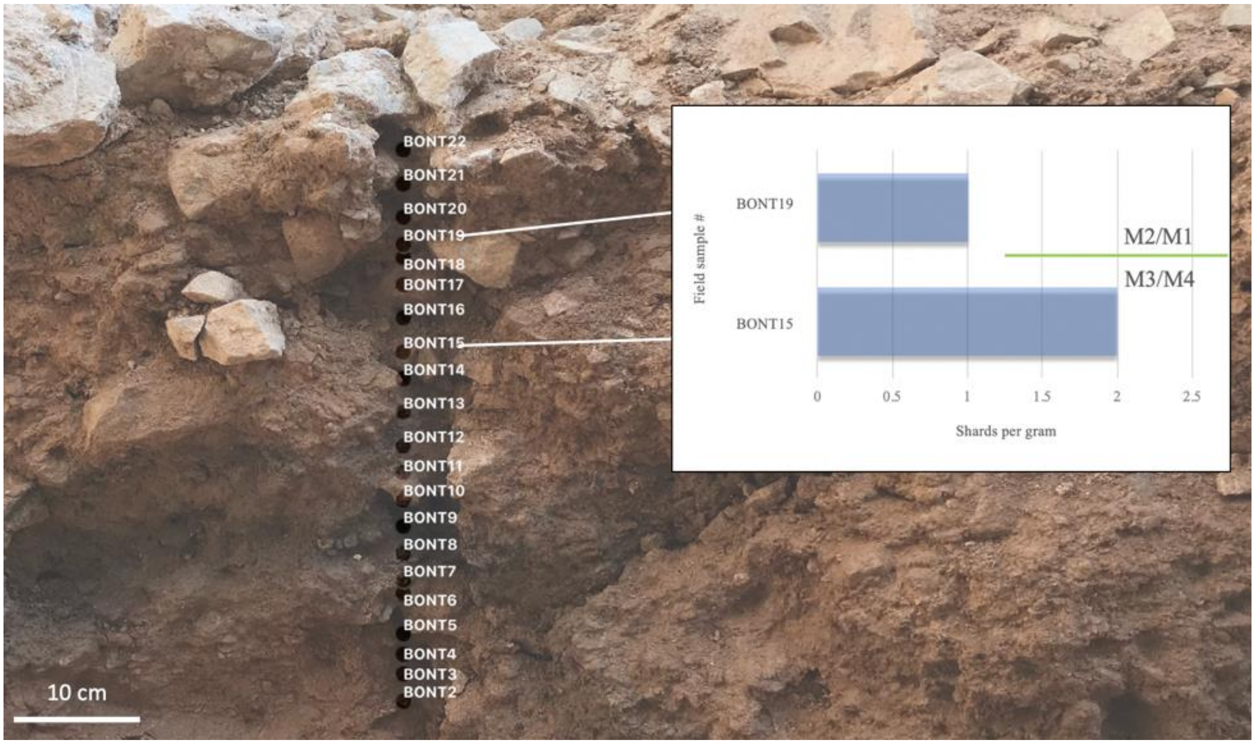

Figure 6. Shard concentrations at Riparo Bombrini. Samples BONT15 to BONT19 are attributed to population three and are present in stratigraphic units M1-M4. The y-axis represents each sample number and the x-axis shows shards per gram.

Table 1. Major (wt.%) element compositions for individual glass shards from Arma Veirana (AV) and Riparo Bombrini (RB). Major element totals are normalized to 100 wt. %. The analytical total before normalization is given. Sample names represent site, sample number, and individual shard. Samples AV651, AV653, and AV662 show compositions for different shards within that sample (e.g. AV651-1 and AV651-2). Sample AV665 shows two analyses for the same shard (i.e. AV 665-2-1 and AV665-2-2).

						Population one					
	AV651-1	AV651-2	AV651-3	AV651-4	AV652-1	AV653-1	AV653-2	AV653-3	AV653-4	AV655-1	AV656-1

SiO_2	76.19	76.60	75.99	76.81	77.46	76.69	75.87	77.18	76.68	76.70	75.09
TiO_2	0.08	0.00	0.14	0.20	0.04	0.00	0.22	0.12	0.17	0.02	0.05
Al_2O_3	13.18	13.01	12.94	12.66	11.60	12.99	12.71	12.49	12.73	12.93	13.47
Cr_2O_3	0.00	0.10	0.00	0.07	0.00	0.00	0.09	0.00	0.01	0.03	0.00
FeO	0.72	0.58	0.79	0.61	0.50	0.73	0.79	0.44	0.73	0.60	0.79
MnO	0.07	0.10	0.08	0.05	0.00	0.02	0.05	0.09	0.07	0.03	0.05
MgO	0.02	0.01	0.03	0.02	0.01	0.04	0.02	0.06	0.04	0.00	0.00
CaO	0.78	0.92	0.99	0.95	0.90	1.00	1.05	0.56	0.89	0.84	1.05
Na_2O	3.61	3.35	3.97	3.60	3.74	3.52	3.41	3.87	3.49	3.69	3.70
K_2O	4.81	5.02	5.05	4.92	4.95	4.93	5.37	4.68	4.80	4.78	5.01
P_2O_5	0.00	0.00	0.00	0.00	0.00	0.00	0.00	0.00	0.00	0.00	0.78
F	0.29	0.22	0.00	0.00	0.33	0.00	0.33	0.17	0.27	0.29	0.00
Cl	0.08	0.06	0.01	0.06	0.08	0.08	0.07	0.04	0.09	0.08	0.00
SO_3	0.00	0.01	0.00	0.04	0.02	0.00	0.01	0.01	0.02	0.01	0.00
BaO	0.15	0.00	0.00	0.00	0.35	0.00	0.00	0.28	0.00	0.00	0.00
Total	98.68	96.60	97.26	96.91	96.17	96.12	97.06	97.68	97.44	99.13	99.97

Table 1 (continued)

	Population one						Population two		Population three		
	AV661-1	AV662-1	AV662-2	AV662-3	AV662-4	AV662-5	AV665-2-1	AV665-2-2	RB15a-1	RB15a-2	RB19a-1
SiO_2	76.51	78.32	77.71	76.54	77.49	77.52	75.78	76.82	76.96	76.84	76.64
TiO_2	0.02	0.00	0.00	0.11	0.00	0.08	0.28	0.38	0.04	0.00	0.00
Al_2O_3	13.17	12.09	12.52	12.71	12.64	12.00	12.27	11.27	11.79	12.31	12.44
Cr_2O_3	0.00	0.04	0.00	0.13	0.00	0.00	0.00	0.00	0.00	0.00	0.00
FeO	0.73	0.47	0.61	0.91	0.61	0.84	2.33	2.65	0.70	0.84	0.89
MnO	0.00	0.05	0.00	0.00	0.11	0.04	0.00	0.10	0.11	0.03	0.10
MgO	0.03	0.01	0.02	0.00	0.00	0.03	0.07	0.09	0.00	0.01	0.02
CaO	0.80	0.47	0.48	0.78	0.42	0.92	0.81	0.87	0.56	0.83	0.70
Na_2O	3.49	3.40	3.67	3.56	4.01	3.24	3.04	2.88	3.30	3.95	4.38
K_2O	4.78	5.03	4.70	4.69	4.53	5.06	5.33	4.72	5.41	4.62	4.51
P_2O_5	0.00	0.00	0.00	0.00	0.00	0.00	0.00	0.08	0.01	0.00	0.00
F	0.28	0.07	0.24	0.48	0.07	0.07	0.00	0.11	0.89	0.28	0.20
Cl	0.09	0.05	0.05	0.07	0.07	0.09	0.09	0.03	0.15	0.22	0.11
SO_3	0.00	0.00	0.00	0.01	0.02	0.12	0.00	0.02	0.07	0.07	0.00
BaO	0.10	0.00	0.01	0.00	0.01	NA	0.00	0.00	NA	NA	NA
Total	96.41	96.47	97.31	98.01	96.17	96.09	93.99	93.10	94	94.31	96.15

Table 2. Trace (ppm) element compositions for Arma Veirana and Riparo Bombrini glass shards.

	Population one				Population two
AV653-1	AV653-2	AV653-3	AV653-4	AV656-1	AV665-2-1

Ga	16.61	21.23	18.51	17.62	19.48	41.73
Rb	197.06	268.84	249.02	246.09	287.81	256.96
Sr	3.90	9.16	9.69	10.20	8.27	62.44
Y	35.41	62.93	61.80	53.93	64.78	94.01
Zr	82.16	128.88	130.14	110.68	101.16	956.35
Nb	54.09	30.86	30.46	27.28	33.72	78.59
Cs	4.80	6.38	4.02	3.99	5.21	6.75
Ba	6.98	4.03	3.86	6.26	0.00	1730.95
La	21.16	17.63	16.57	15.13	12.56	128.26
Ce	40.40	40.47	38.44	38.45	31.47	300.20
Pr	4.03	5.36	6.22	6.08	4.84	32.28
Nd	17.40	22.45	19.99	22.18	19.03	118.22
Sm	4.66	7.87	5.01	5.24	6.09	28.85
Eu	0.00	0.27	0.54	0.06	0.27	3.09
Gd	2.47	8.17	6.25	5.17	6.68	21.34
Tb	0.90	1.21	1.35	1.20	1.20	4.36
Dy	4.44	8.61	8.03	7.82	8.53	21.33
Ho	0.76	1.83	1.62	1.74	1.81	4.51
Er	2.76	6.05	5.40	5.41	6.13	14.90
Tm	0.47	0.79	1.19	0.97	1.12	1.90
Yb	2.29	7.76	6.59	6.84	7.34	14.08
Lu	0.44	1.52	1.15	1.09	1.19	1.96
Hf	3.71	5.79	5.39	4.50	4.91	25.43
Ta	6.77	2.72	2.60	3.10	2.87	7.14
Pb	32.77	37.44	33.42	35.41	39.80	29.53
Th	20.28	29.18	32.16	27.21	27.66	29.39
U	8.03	5.83	5.05	6.35	6.82	6.53

Table 2 (continued).

	Population three					
	RB15a-1-1	RB15a-1-2	RB15a-2 1	RB15a-2-2	RB19a-1-1	RB19a-1-2
Ga	14.39	17.17	24.23	14.40	20.26	17.49
Rb	247.88	306.60	367.33	339.58	280.95	289.99
Sr	3.82	3.44	4.68	18.12	2.61	4.22
Y	83.08	104.96	171.19	121.20	91.82	99.13
Zr	118.46	132.21	155.57	169.52	122.58	133.33
Nb	39.04	43.59	50.43	37.42	39.68	40.91
Cs	6.81	7.70	7.84	7.96	7.32	7.46
Ba	2.03	1.41	4.06	14.17	0.67	2.51
La	8.48	10.89	9.86	5.52	11.45	11.15
Ce	25.07	30.63	26.25	20.57	31.82	31.78
Pr	3.16	3.86	3.29	1.83	4.96	4.07
Nd	18.00	20.55	12.78	15.78	21.44	21.51
Sm	6.66	6.85	10.62	8.11	7.76	7.77
Eu	0.00	0.00	0.00	0.26	0.12	0.00
Gd	6.76	9.66	11.99	11.15	9.44	8.23
Tb	1.43	1.76	2.15	2.44	1.52	1.81
Dy	11.22	14.07	19.19	16.40	12.66	11.62
Ho	2.60	3.02	3.77	5.42	2.96	2.88
Er	8.96	10.99	17.30	12.65	10.27	10.30
Tm	1.39	1.68	2.57	13.48	1.70	1.58
Yb	8.88	11.87	22.07	56.76	11.69	11.71
Lu	1.57	1.75	2.77	1.80	1.88	1.63
Hf	5.78	6.51	8.96	11.21	7.37	6.88
Ta	3.74	3.53	4.40	3.61	4.29	4.10
Pb	35.03	40.86	37.93	41.42	44.73	38.06
Th	27.79	33.61	40.77	35.87	34.57	33.99
U	6.98	8.89	9.21	8.67	9.07	7.91

5. Source of the shards

5.1 Locating potential sources

P1 shards (Arma Veirana) and P3 shards (Riparo Bombrini) are nearly identical in major and trace element composition and are probably related to the same eruptive event, so we group them for the purpose of locating a source and will refer to them as P1,3. P2 shows a very distinct geochemical signature that is likely derived from an eruption in a different region. P1,3 shards are high silica, calc-alkaline rhyolite with FeO<1 wt. % and K2O/Na2O >1 and are atypical of rhyolite erupted from volcanoes in the Mediterranean region. The shards lack a distinctive Nb-Ta trough characteristic of subduction zone magmatism and are more typical of intraplate volcanism. P2 shards are also high silica, calc-alkaline rhyolites but with 2.33-2.65 wt.% FeO. Magmatic provinces in Italy, except those in the Aeolian Islands, are mainly subduction related and tend to be alkalic to ultrapotassic and have higher FeO and light rare earth element (LREE) concentrations than AV or RB shards (Peccerillo, 2005). Other areas in the Mediterranean (i.e. Aegean Sea, Marmara Sea, Greece) are also dominated by subduction zones and show significant differences in trace elements when compared to P1,3 and P2 (Aksu *et al.*, 2008; Tomlinson *et al.*, 2012; Satow *et al.*, 2015; Koutrouli *et al.*, 2018). The tectonic setting of Lipari Island in the Aeolian Island chain is somewhat controversial. Chiarabba et al. (2008) suggest that Aeolian Island volcanism is related to post-subduction back-arc extension with an inactive subducted slab at depth. The REE signature of P1,3 is very distinctive with depleted LREE, a deep Eu anomaly and enriched HREE. This signature is very rare and is found in rhyolites with high fluorine content that have undergone extensive crystal fractionation (Christiansen et al. 2007; Jowitt et al. 2017) or created by fractionation of rare-earth bearing minerals like Allanite (Miller and Mittlefehldt, 1982). Many of these rhyolites are associated with economic mineral deposits (reviewed in Jowitt et al. 2017). The Ba, Sr and Eu troughs are due to fractionation of feldspar, suggesting that the source volcano is compositionally zoned. The trace element signature for P2 show enriched LREE and follow similar trends to volcanoes on the western and eastern side of Iceland, which are located along the axis of a rift (Jakobsson and Jónasson et al., 2008).

Based on the geochemistry of the shards and lack of similar proximal sources, locating a source volcanic eruption for Arma Veirana and Riparo Bombrini P1,3 and P2 shards required a worldwide search for eruptions with a comparable major and trace element chemistry (Table S1 and Table S2). Ideally, major and trace element chemistry should be sufficient to match cryptotephra to a source, but in the case of P1,3, several volcanic areas are candidate sources and because most analyses for the comparison volcanoes are whole rock and not glass, we considered other factors such as age of the enclosing sediments, shape and freshness of shards, and ease of transport from the source volcano to the site of deposition in our search for a source. We searched for eruptions in a variety of tectonic settings and, due to the poor age constraint at AV and RB, we included a wide range of ages in our search (Table S1 and Table S2). Important parameters for a chemical match of P1,3 shards to a possible source are SiO_2>75 wt. %, FeO<1 wt. %, K_2O/Na_2O>1, primitive mantle normalized Nb/Ta<1, depletion in Ba, Sr, Eu, and LREE and enrichment in U, Th compared to primitive mantle. Parameters for a chemical match of P2 shards are SiO_2>75 wt. %, FeO>2 wt. %, K_2O/Na_2O>1, depletion in Sr and Eu and an enrichment in LREE to primitive mantle. After the worldwide search, we narrowed the list of possible sources for P1,3 shards to three volcanic fields and two volcanoes for P2. P1,3 possible sources are the Acigöl volcanic field in Turkey, and the Kirka-Phrigian Caldera in central Turkey and eruptions on Lipari Island, Italy, and P2 possible sources are Öraefajökull or Torfajökull in Iceland.

5.2 Statistically distinguishing sources

Add Bayesian results here when Jake is finished*

5.3 Acigöl Complex, Anatolia

The Acigöl Complex, located in central Anatolia, is similar in major and trace compositions to P1,3 (Fig 7 and Fig 8). Various eruptions and deposits of the Acigol Complex were examined as potential sources (i.e. Young Dome, Korudag, Bogazköy, lower Acigöl Tuff, upper Acigöl Tuff, Kaleci, Tepeköy, Guneydag, Kuzay, and Karniyarik) that range in age from 180 ka to 20 ka. While the data are scarce (Druitt et al., 1995; Siebel et al., 2011), the compositions of some of the younger eruptions (i.e. Karniyarik, Guneydag, Kuzay) are closer in major and trace composition to P1,3 than the older eruptions (i.e. lower Acigöl Tuff, upper Acigöl Tuff, Bogazköy). Both major and trace element concentrations for the younger (20 ka) eruptions in the Acigöl volcanic field match P1,3 chemistry, but several factors rule out this area as source: First, the eruptions occurred during tuff-ring formation prior to the extrusion of rhyolite domes. These eruptions were low volume and unlikely to spread tephra far from the source (Axel Schmitt, personal communication). Second, tephra transport from Turkey to Italy is east to west against prevailing atmospheric circulation. We suggest that transport of low-volume tephra in this direction is unlikely. Third, trace element chemistry was analyzed by X-ray fluorescence spectrometry and not LA-ICP-MS. Although these data may be reliable, it is not appropriate to compare datasets obtained by different analytical methods. Therefore, we rule out eruptions from the Acigöl Complex as the source of P1,3 shards.

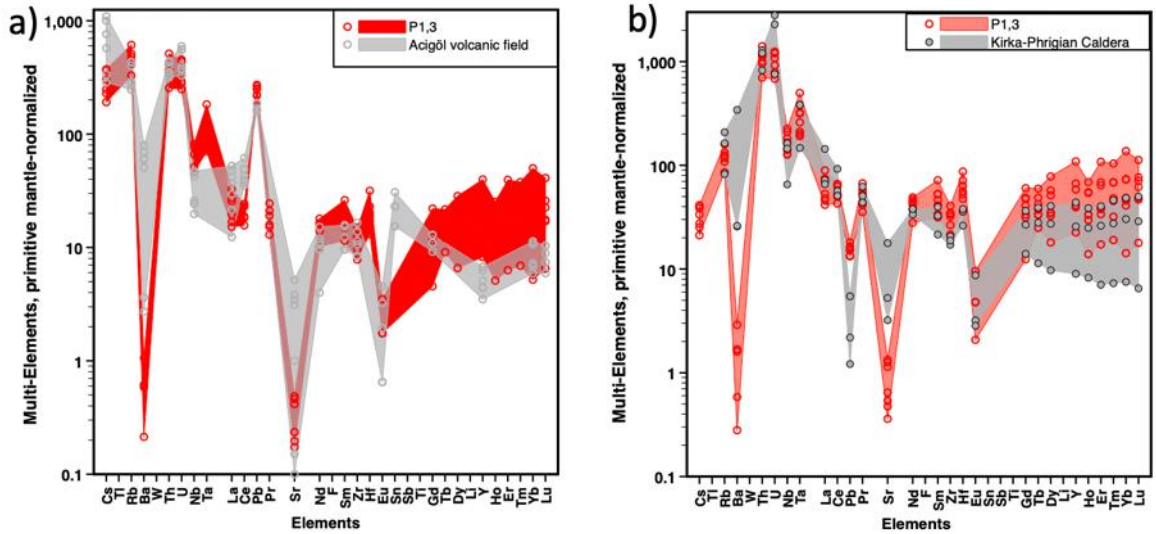

Figure 7 Geochemical comparisons of P1,3 and potential sources. a), Comparison of trace element chemistry of P1,3 shards to rhyolite from Acigöl volcanic field. Trace element data is normalized to primitive mantles of Sun and McDonough (1989). **b)**, Comparison of trace element chemistry of P1,3 shards to rhyolite from Kirka-Phrigian caldera. Trace element data is normalized to primitive mantles of Sun and McDonough (1989).

5.4 Kirka-Phrigian, Anatolia

We also considered the possibility that P1,3 shards were reworked from local sedimentary rocks that contain tephra from Miocene eruptions. One possible source of Miocene shards is ash-flow tuff erupted during the formation of the Kirka-Phrigian Caldera in western Anatolia at about 18 Ma (Seghedi and Helvac, 2016). Both major and trace elements whole-rock data provide an excellent match to P1,3 (Fig 7 and Fig 8) and it is possible that a caldera forming event of this magnitude could have spread tephra across Europe. However, this match is based on a comparison of glass to whole rock data and glass analyses for the Kirka-Phrigian tuffs are required to make a more robust correlation. Additionally, there are various factors that rule out

Kirka-Phrigian as a source for P1,3. Transport of tephra from Kirka-Phrigian to Italy involves a complex series of events. The incorporation of Kirka-Phrigian shards in AV-RB sediment would require that the caldera eruption spread tephra across Europe in the Miocene. Then, the tephra would have to be stored in Miocene sediments like those described in western Italy in the Po Valley (Ruffini, Cadoppi and D'Atri, 1995). Last, shards would have to be eroded from these deposits, transported and deposited at AV and RB simultaneously. We consider this sequence of events very unlikely. Shards are delicate and easily altered and thus would likely lose their delicate angular sharp edges and vitric interiors if subjected to long distance transport by alluvial, aeolian, and soil formation processes.

5.5 Lipari Island

The Lipari Volcanic complex in the Aeolian Islands formed between 267 ka and AD 776 to 1220 (Forni *et al.*, 2013). Volcanoes erupted calc-alkaline basaltic andesite to rhyolite with rhyolite being dominant for the last 43 ka. Eruptions from two of these volcanoes; Falcone (43-40 ka) and Punta del Perciato (56-43 ka) produced chemically identical high-silica rhyolite domes and pyroclastic deposits and are candidate sources for P1,3 shards. We compared trace elements of P1,3 to tephra produced by Falcone and Punta del Perciato volcanoes (FPelP) compiled by Albert et al. (2017). Using a multielement plot normalized to primitive mantle (Fig 8) both P1,3 and FPdelP tephra show depletion in Ba, Sr, and Eu suggesting magmatic fractionation of feldspar (most likely K-feldspar). Both have Nb/Ta<1 and enriched U contents. P1,3, however, is depleted in light rare-earth elements (REE) and slightly enriched in heavy REE compared to FPdelP. Also, Th is lower in P1,3 than FPdelP. REE differences at first appear to invalidate a correlation between FPdelP and P1,3 but may be explained if P1,3 represents a highly fractionated explosive phase of the FPdelP eruption. A common way of producing light REE depletion in rhyolite is mineral fractionation of REE-rich accessory minerals like Allanite and Monazite and to a lesser extent apatite and zircon (Miller and Mittlefehldt, 1982). Both Allanite and Monazite become saturated in rhyolitic magma at low concentrations, and because of their small size and low abundance, they are easily overlooked in thin sections using traditional optical methods. Allanite and Monazite fractionation occur in the upper more highly fractionated and volatile-rich part of a magma chamber that is erupted explosively early in an eruption (Miller and Mittlefehldt, 1982). Shards produced by such an eruption would be carried in the eruptive plume and eventually distally deposited. This event may not be recorded in proximal deposits. We suggest that the light REE depletion in P1,3 formed in this manner and that P1,3 represents a highly fractionated early erupted component of the eruption related to FPdelP.

An example of a tephra unit erupted from Lipari but not recorded in the stratigraphic record on the island is unit E-11, the oldest tephra deposit in Tyrrhenian Sea Marine Core KET8003 (Paterne, Guichard and Labeyrie, 1988). The tephra is dated to 37.7 ka, it occurs directly above the 39 ka Campanian Ignimbrite (CI) (De Vivo *et al.*, 2001), and it may be a widespread marker bed (Albert *et al.*, 2017) also found in the Ionia Sea as unit T1535 (Matthews *et al.*, 2015) and I-2 (Insinga *et al.*, 2014). Although only major element chemistry is available for tephra from these marine core units, they are most likely associated with the FPdelP volcanoes on Lipari Island (Albert *et al.*, 2017). Major elements for E-11, T1535 and I-2 are similar to P1,3 (Fig 8). All are high silica, low FeO rhyolites with $K_2O/Na_2O>1$. CaO concentrations are lower than P1,3 but fall within one standard deviation of mean P1,3 values. Overall this marine core tephra compares well with P1,3. Albert et al. (2017) ruled out a direct correlation with proximal units because FPdelP rhyolites are more elevated in K_2O than E-11 and both are older than E-11 and predate the CI, whereas E-11 overlies the CI (Albert *et al.*, 2017). Albert et al. (2017) suggest that E-11 may represent a younger eruption from Falcone, but all evidence of this eruption on Lipari was erased by even younger eruptions from Monte Guardia. Therefore, the tephra record in the marine core may provide a better historical eruption record than found proximally on Lipari.

Eruptions from Lipari Island are the most likely source for P1,3 for the following reasons: First, the age of eruptions (56-37.7 ka) is compatible with the age assumed for sediments at Riparo Bombrini and Arma Veirana. Second, northward transport of tephra from Lipari to northwest Italy is well documented. In fact, E-11 is found in the marine core to the north of Lipari Island and T1535 and I-2 in the Ionian Sea. Third, the chemical match between FPdelP and E-11 and P1,3 is not perfect, but major elements are very similar and as discussed, P1,3 may represent an early explosive phase related to the FPdelP event. Unfortunately, the record of eruptive events on Lipari Island is incomplete due to erosion or non-deposition, so there is no record of this explosive phase on Lipari Island. Despite the incomplete record, the 56-37.7 ka Lipari eruptions still represent the best match to P1,3 based on age, compatibility with the age of Arma Veriana and Riparo Bombrini sediments, ease of transport, and chemistry. Determining the specific Lipari eruption responsible for P1,3 is a major objective. Future work will focus on obtaining trace elements on glass shards associated with FPdelP dome eruptions and marine core samples.

Table 3. Major element chemistry of possible sources and comparison to P1,3.

	E-11*	T1535**	I-2***	Mean P1	SDEV[&]	Mean P3	SDEV[&]	Falcone[%]	Puna del Perciato[%]
SiO_2	76.73	76.92	76.56	76.81	0.79	76.59	0.49	76.28	76.47
$Ti0_2$	0.06	0.09	0.06	0.07	0.45	0.04	0.04	0.19	0.04
$A1_20_3$	13.04	12.40	12.76	12.75	0.04	12.46	0.32	12.44	12.36
FeO#	1.01	1.31	1.35	0.66	0.13	0.93	0.19	1.50	1.16
MgO	0.06	0.02	0.05	0.05	0.02	0.01	0.01	0.01	0.01
CaO	0.65	0.65	0.71	0.81	0.21	0.80	0.18	0.72	0.69
Na_20	3.27	3.73	3.49	3.63	0.20	4.00	0.31	3.33	3.37
K_2O	5.05	4.84	4.97	4.88	0.20	4.79	0.39	5.60	5.77
Total	99.87	97.32	99.61					95.34	95.64

*E-11 (Paterne et al. 1988)
**T1535 (Matthews et al. 2015)
***I-2 (Insinga et al. 2014)
[%]Falcone and Puna del Perciato (Albert et al. 2017)
#For E-11, reported as Fe2O3 converted to FeO
[&]SDEV=one standard deviation
Total is pre-normalization analytical total

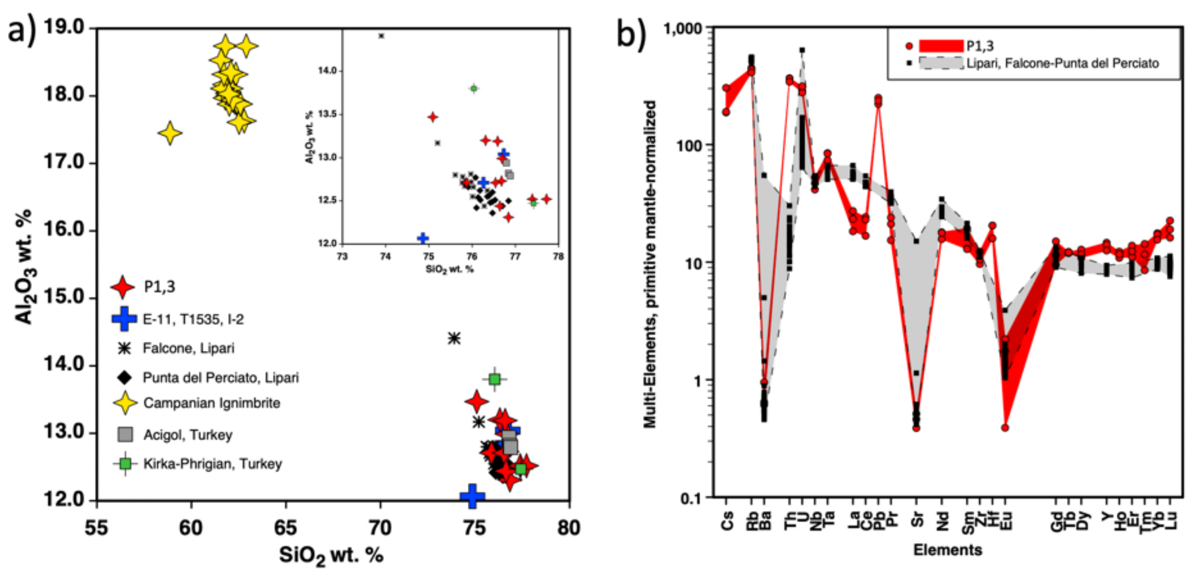

Figure 8. Geochemical comparisons of P1,3 and potential sources. a), SiO_2 vs Al_2O_3 (weight percent, wt%). Plot in top right corner is excluding the Campanian Ignimbrite. **b)**, Comparison of trace element chemistry of P1,3 shards to rhyolite from Falcone Volcano, Lipari and Punta del Perciato (data from Albert et al. (2017)). Trace element data is normalized to primitive mantles of Sun and McDonough (1989).

5.6 Öraefajökull and Torfajökull, Iceland

The same potential sources were examined for P2 as P1,3. Some sources were easily eliminated due to the higher FeO values (>2 wt.%) and different trace element values that P2. For P2, the most probable source eruptions are from Iceland (Fig 9). Multiple tephra deposits from a marine core collected in the North Atlantic show geochemical similarities to P2 (Abbott *et al.*, 2014). Deposits range in age from MIS 6 to MIS 4 (190-70 ka) and have been linked with nearby cores (i.e. ENAM33). Potential source volcanoes are Öraefajökull or Torfajökull; however, exact eruptions are not yet determined. Compositions from various deposits throughout Iceland were also considered (Jónasson, 2007; Martin and Sigmarsson, 2007). Data from these analyses show similarities in trace elements for Torfajökull and P2, further confirming this area as a source (Fig 9). The primitive-mantle plot (Fig. 9) shows that both Torfajökull and P2 are slightly depleted in Cs, Rb, Ba, Th and U. Therefore, the shards from P2 could have originated from Torfajökull, but we have not identified the exact eruption. Further investigations will focus in this region.

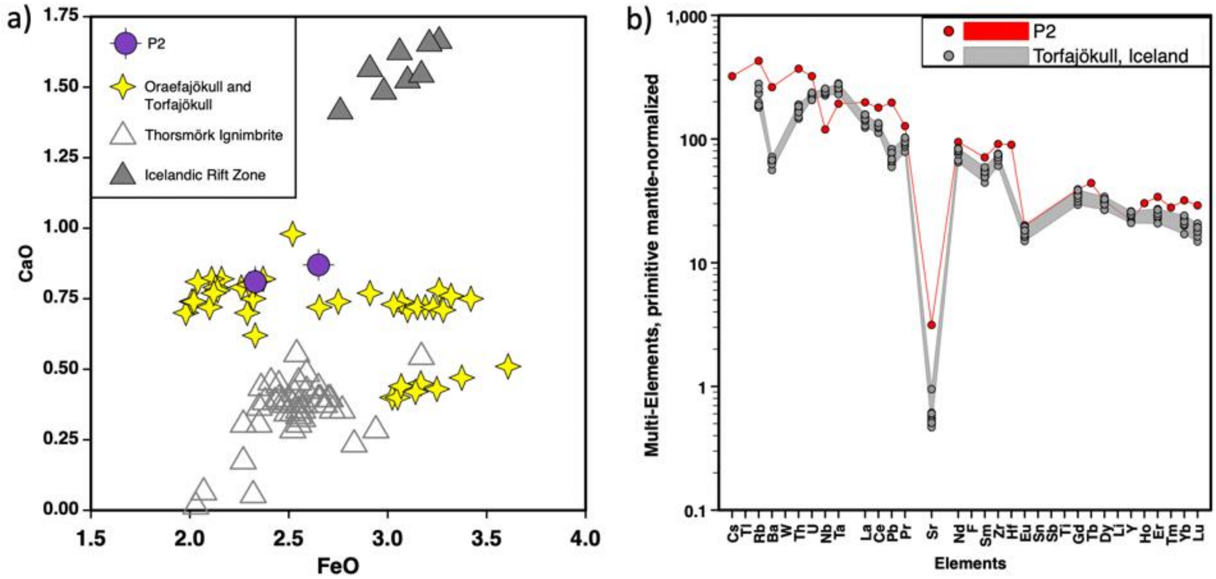

Figure 9. Geochemical comparison of P2 and potential sources. a), FeO vs. CaO (weight percent, wt%). Data is retrieved from Abbott et al. (2014), Martin and Sigmarsson (2007) and Tomlinson et al. (2010). **b),** Trace element chemistry of P2 shards to rhyolite from Torfajökull (data from Abbott et al. (2014)). Trace element data is normalized to primitive mantles of Sun and McDonough (1989).

5.7 Distinguishing primary and reworked tephra

There is currently little known about post-depositional processes of tephra within cave or rock shelters due to the rarity of these finds (Housley and Gamble, 2015). More focus has been placed on understanding secondary deposition, reworking and density movement through peatlands and lacustrine deposits (Boygle, 1999; Beierle and Bond, 2002; Payne and Gehrels, 2010). This is an obvious area that needs to be explored for cave and rock shelter deposits; however, for the time being, examining shard count profiles is the primary method. When dealing with extremely low abundance shards, micromorphological analyses are also useful to better understand the amount of reworking between stratigraphic units as well as how the deposits accumulated at each site (Smith et al., 2018). This aides in quantifying what depositional and post-depositional processes may have affected the shards. Therefore, a more reliable tephra location can be determined based on shard count profiles and micromorphological analyses and has been employed in this study.

A shard count profile was only developed for P1 and P3 (Fig 4 and 5) due to extremely low abundance (<4 shards/gram) for P2. Shards from P2 at Arma Veirana were only present in one sample (AV665) from stratigraphic unit Gr. Therefore, we assign a tentative isochron location of P2 to stratigraphic unit Gr until more shards are discovered. The shard count profile for P1 at Arma Veirana displays a few distinct peaks present in the BM and Gr, with the vast majority of shards present in the BM. Because the highest shard count is at the base of the section, it is possible that more shards continue below the collected section which has not been exposed yet. Micromorphological analyses at Arma Veirana show a large amount of anthropogenic input present in stratigraphic unit BM. However, Unit Gr shows less anthropogenic influence and no clear signs of bioturbation implying it is the least disturbed. The contact between these stratigraphic units appears sharp in the field. Under the microscope, the contact appears more diffuse, but only on the order of 1-2 centimeters, demonstrating that there is no significant mixing between these layers. Both Gr and BM consist of a mixture of material, suggesting formation by colluviation and roof-fall. It is likely shard deposition occurred via aeolian processes. Because the highest shard count is present in the BM, we give a tentative isochron location of P1 to stratigraphic unit BM, with the assumption that shards continue further down the unexposed section. It is important to note that the presence of P1 shards in the Gr is likely due to slight reworking of shards and is not because they were primarily deposited in that unit, which has been supported by the micromorphological analyses. Further excavation and sampling will help determine the earliest stratigraphic appearance of P1 at Arma Veirana.

The shard count profile for P3 at Riparo Bombrini displays one peak present in stratigraphic M4/M3 (Fig 6). Micromorphological analyses at Riparo Bombrini show minimal bioturbation or reworking of the sediments. Mineral constituents in each micromorphology sample contain aeolian and volcanic materials, which do not belong to the geology of the rock shelter, suggesting they were secondarily deposited (i.e. wind-blown). The aeolian and volcanic materials were potentially reworked from older sediments and deposited via wind deflation of the shelf, which was exposed in the Upper Pleistocene. It is likely that shards entered the cave during the deposition of these aeolian materials. Because shard abundance is extremely low, we assign a tentative location of the isochron for P3 to stratigraphic units M4/M3 and more shards need to be discovered to obtain a confident location. While the exact stratigraphic location of shards is still under investigation, we have obtained a rare composition at both sites which has the potential to be used as a link between deposits between AV and RB as well as other Middle-Upper Paleolithic sites throughout the region. This study also demonstrates that cave and rock shelter sites can work as archives of cryptotephra and we need to always examine these areas, despite the rarity of shards (Housley and Gamble, 2015).

6. Pitfalls

6.1 Comparing data from different labs

Compiling compositional data from published sources can be difficult due to the differences in how worldwide laboratories analyze and report chemistry. While the development of large-scale databases (e.g. the RESET Project, VOGRIPA, Tephrabase) are critical steps forward, differences in the type of materials analyzed make it difficult to directly compare data from various sources. While analytical conditions are often reported, variations in analytical techniques must be taken into consideration when comparing data. Additionally, caution is needed when comparing whole-rock data to glass data, as results can fluctuate depending on the amount of crystals present in the whole-rock samples. If the percentage is small, then the whole-rock should be very similar to glass data (White, 2013). However, glasses can contain compositional heterogeneity that is sometimes not preserved in whole-rock samples and when compared, glass chemistry will be depleted in compatible elements and enriched in incompatible elements (Tomlinson *et al.*, 2015). To account for this issue, examining trace ratios like Ba/Nb can be helpful. If the phenocrysts are in equilibrium with the liquid, this ratio should stay consistent in both liquid and crystals, providing a temporary solution until more data are available. Therefore, the potential sources we suggest in this study are not concrete correlations and will not be confirmed until glass data is provided.

6.2 Correlation issue

The Middle-Upper Paleolithic transition is a difficult period to date. Currently, most sites that preserve these records have been dated using radiocarbon (reference); however, the dating limit of radiocarbon (50-40 ka) falls right at the middle of that transition (Higham, 2011). Moreover, radiocarbon dates are commonly susceptible to contamination and can result in underestimations of the real age (Higham, 2011). Despite methodological advancements (Higham et al. 2014), the issues surrounding radiocarbon dating near its limit require archaeologists to use complimentary dating and correlation methods. In this study, we noted the complications with the radiocarbon dates from Arma Veirana and Riparo Bombrini. Dates at

Arma Veirana vary from near the dating limit of radiocarbon and beyond, whereas some dates at Riparo Bombrini show underestimations of the expected calculated age based on the cultural sequences (i.e. M2, M3 and M5). Therefore, radiocarbon dates cannot be used to test the amount of overlap between deposits. While this does not mean calculated dates are necessarily wrong, it simply calls for another method to correlate the deposits and further test the proposed chronologies. In this study, we use cryptotephra as a supplementary method to correlate deposits at Arma Veirana and Riparo Bombrini, given both sites have deposits close to the dating limit of radiocarbon.

Cryptotephra investigations in this study show that P1 at Arma Veirana is the same as P3 at Riparo Bombrini, providing a potential marker horizon between deposits at both sites. With this correlation, there are a few factors that need to be considered between both sites. First, Arma Veirana and Riparo Bombrini preserve two different depositional environments, which means the introduction of shards may have been at different times. While shards are present in two technologically similar units at both sites, suggesting they were introduced during the same time, these are important factors to keep in mind. Second, an exact isochron location has not yet been identified. This is due to the extremely low abundance (<4 shards/gram) of shards for P3 at Riparo Bombrini and the possibility that P1 shards at Arma Veirana continue further down the unexcavated section. This will be critical in providing an exact link between both sites. More cryptotephra samples need to be collected in order to solve both of these issues. Despite these issues, we have identified a new composition that has not yet been reported in archaeological sites in the Mediterranean region and it is in deposits that are close to the dating limit of radiocarbon. Once the isochron location is refined, this marker horizon can be used to test calculated dates (i.e. radiocarbon) as well as further refine correlations between archaeological sites throughout the Mediterranean region during the Middle-Upper Paleolithic transition.

7. Conclusions

The use of cryptotephra in archaeological studies is advancing how scientists date and correlate archaeological sites over large distances. Tephra studies have become especially important as many sites rely on radiocarbon dating even when deposits are close to the limit of this method (50-40 ka). In this contribution, we used tephrochronology to correlate the occupational histories at two Middle-Upper Paleolithic sites, Arma Veirana and Riparo Bombrini. These sites are located 80 km apart and contain similar cultural industries, suggesting potential overlap between deposits. We sampled both sites with the goal of finding shards of the same composition, allowing for a direct comparison of deposits. We also integrated micromorphological studies in order to better understand the depositional and post-depositional processes that may have affected the location of shards.

Our work resulted in the discovery of two shard populations (P1 and P2) at Arma Veirana and one population (P3) at Riparo Bombrini. Geochemical analyses showed that P1 is from the same eruption as P3, providing a unique marker between deposits. We suggest P1,3 shards represent a highly fractionated early erupted component of 37.7-56 ka rhyolite from Lipari Island, however, because no glass shard data is available for Lipari deposits, these conclusions are tentative. P2 shards show a depletion in Sr and an enrichment in LREE which is likely derived from Torfajökull in Iceland; however, we have not identified the exact eruption. The most important result is the identification of P1,3 at both Arma Veirana and Riparo Bombrini, allowing for a tool to test the amount of overlap between deposits. As discussed above, the exact isochron location is not yet determined due to extremely low abundance (<4 shards/gram) of shards in P3 and uncertainty regarding the distribution of shards in P1. Micromorphological results show minimal reworking at both sites, suggesting the location of shards are reliable. Despite these results, more shards need to be identified to refine the isochron and future excavations will focus on this.

This study highlights how cryptotephra can be used to link archaeological deposits and test the validity of other dating methods even without identifying a specific source eruption. The chemistry of P1,3 shards is distinctive and unusual for European volcanoes suggesting there is still more work that needs to be done in this region. This particular marker will be important for asking questions pertaining to the Middle-Upper Paleolithic transition and correlating other Paleolithic sites throughout Europe.

Data Availability

Table S1 – List of reference tephra

Table S2- Compiled data used for sourcing tephra

Acknowledgements

This research would not have been possible without the help of various researchers and students. Daniel Veres from the Romanian Academy, Institute of Speleology and David Karáston from Eötvös University, Department of Physical Geography provided samples from Ciomadul Complex. Victoria Smith from the Research Laboratory for Archaeology and the History of Art at University of Oxford and Helge Arz from Leibnitz Institute for Baltic Sea Research in Germany provided samples from the Black Sea Core. Harangi Szabolcs from Eötvös University, Department of Physical Geography provided trace element data from Ciomadul Complex. Sabine Wulf from the University of Portsmouth, Department of Geography and Axel Schmitt from the Universitát Heidelberg provided helpful information regarding potential sources. Chris Campisano, Michael Barton, John Murray and Andrew Zipkin from Arizona State University provided helpful guidance and edits on this paper.

Author Contribution

J.H., C.O., F.N., J.R., D.S., M.P, S.B, and C.G. co-supervised excavations at Arma Veirana. J.R. and F.N. co-supervised excavations at Riparo Bombrini. J.N.H. collected cryptotephra samples at Arma Veirana and Riparo Bombrini. J.N.H., R.J. and S.F. processed cryptotephra samples at the University of Nevada, Las Vegas. M.R. analyzed shards by EPMA at the University of Nevada, Las Vegas. E.S. supervised all cryptotephra analyses. Excavators supervised under J.H. and C.O. sampled for radiocarbon samples at Arma Veirana. J.H. and C.O. chose radiocarbon samples to send to Oxford University for analyses. J.A.H. completed statistical analyses on the compositions of shards. C.E.M. conducted micromorphological analyses at Arma Veirana and A.Z. and G.S.M conducted micromorphological analyses at Riparo Bombrini. C.W.M. and E.S. advised J.N.H and contributed to the direction of this study. J.N.H. and E.S. wrote this text and all authors contributed to edits.

Funding sources

This research was supported by funding from the following agencies and organizations: National Geographic Society, Wenner-Gren Foundation for Anthropological Research; Leakey Foundation; University of Colorado Denver; Washington University; Hyde Family Foundations; the Office of Knowledge Enterprise Development, Graduate Professional and Student Association (GPSA), and the Graduate College at Arizona State University (ASU); and the Cryptotephra Laboratory for Archaeological and Geological Research (CLAGR) at the University of Nevada, Las Vegas (UNLV).

References:

Abbott, P. M. *et al.* (2014) ‘Re-evaluation and extension of the Marine Isotope Stage 5 tephrostratigraphy of the Faroe Islands region: The cryptotephra record’, *Palaeogeography, Palaeoclimatology, Palaeoecology*. The Authors, 409(December 2015), pp. 153–168. doi: 10.1016/j.palaeo.2014.05.004.

Aksu, A. E. *et al.* (2008) ‘Occurrence, stratigraphy and geochemistry of Late Quaternary tephra layers in the Aegean Sea and the Marmara Sea’, *Marine Geology*, 252(3–4), pp. 174–192. doi: 10.1016/j.margeo.2008.04.004.

Albert, P. G. *et al.* (2017) ‘Glass geochemistry of pyroclastic deposits from the Aeolian Islands in the last 50 ka: A proximal database for tephrochronology’, *Journal of Volcanology and Geothermal Research*. Elsevier B.V., 336, pp. 81–107. doi: 10.1016/j.jvolgeores.2017.02.008.

Barton, R. N. E. *et al.* (2014) ‘The role of cryptotephra in refining the chronology of Late Pleistocene human evolution and cultural change in North Africa’, *Quaternary Science Reviews*, 118, pp. 151–169. doi: 10.1016/j.quascirev.2014.09.008.

Beierle, B. and Bond, J. (2002) ‘Density-induced settling of tephra through organic lakesediments’, *Journal of Paleolimnology*. Kluwer Academic Publishers, 28(4), pp. 433–440. doi: 10.1023/A:1021675501346.

Benazzi, S. *et al.* (2015) ‘The makers of the Protoaurignacian and implications for Neandertal extinction’, *Science*, 348(6236), pp. 793–796. doi: 10.1126/science.aaa2773.

Blockley, S. P. E. *et al.* (2005) ‘A new and less destructive laboratory procedure for the physical separation of distal glass tephra shards from sediments’, *Quaternary Science Reviews*, 24(16–17), pp. 1952–1960. doi: 10.1016/j.quascirev.2004.12.008.

Boygle, J. (1999) ‘Variability of tephra in lake and catchment sediments, Svinavatn, Iceland’, *Global and Planetary Change*, 21(1–3), pp. 129–149. doi: 10.1016/S0921-8181(99)00011-9.

Douka, K. *et al.* (2014a) ‘The chronostratigraphy of the Haua Fteah cave (Cyrenaica, northeast Libya)’, *Journal of Human Evolution*. Elsevier Ltd, 66(1), pp. 39–63. doi: 10.1016/j.jhevol.2013.10.001.

Douka, K. *et al.* (2014b) ‘The chronostratigraphy of the Haua Fteah cave (Cyrenaica, northeast Libya)’, *Journal of Human Evolution*. Elsevier Ltd, 66(1), pp. 39–63. doi: 10.1016/j.jhevol.2013.10.001.

Druitt, T. H. *et al.* (1995) ‘Late Quaternary rhyolitic eruptions from the Acigol Complex, central Turkey’, *Journal of the Geological Society*, 152(4), pp. 655–667. doi: 10.1144/gsjgs.152.4.0655.

Forni, F. *et al.* (2013) ‘Chapter 10 Stratigraphy and geological evolution of the Lipari volcanic complex (central Aeolian archipelago)’, *Geological Society, London, Memoirs*, 37(1), pp. 213–279. doi: 10.1144/m37.10.

Harris, J. A. *et al.* (2017) ‘The trajectory of bone surface modification studies in paleoanthropology and a new Bayesian solution to the identification controversy’, *Journal of Human Evolution*, 110, pp. 69–81. doi: 10.1016/j.jhevol.2017.06.011.

Higham, T. (2011) ‘European middle and upper palaeolithic radiocarbon dates are often older than they look: Problems with previous dates and some remedies’, *Antiquity*, 85(327), pp. 235–249. doi: 10.1017/S0003598X00067570.

Higham, T. *et al.* (2014) ‘The timing and spatiotemporal patterning of Neanderthal disappearance’, *Nature*, 512(7514), pp. 306–309. doi: 10.1038/nature13621.

Holt, B. *et al.* (2018) ‘The Middle-Upper Paleolithic transition in Northwest Italy: new evidence from Riparo Bombrini (Balzi Rossi, Liguria, Italy)’, *Quaternary International*. Elsevier, (August), pp. 0–1. doi: 10.1016/J.QUAINT.2018.11.032.

Housley, R. A. and Gamble, C. S. (2015) ‘Examination of Late Palaeolithic archaeological sites in northern Europe for the preservation of cryptotephra layers’, *Quaternary Science Reviews*, 118, pp. 142–150. doi: 10.1016/j.quascirev.2014.05.012.

Insinga, D. D. *et al.* (2014) ‘Tephrochronology of the astronomically-tuned KC01B deep-sea core, Ionian Sea: Insights into the explosive activity of the Central Mediterranean area during the last 200ka’, *Quaternary Science Reviews*. Elsevier Ltd, 85, pp. 63–84. doi: 10.1016/j.quascirev.2013.11.019.

Jakobsson, S. P., Jónasson, K. and Sigurdsson, I. A. (2008) ‘The three igneous rock series of Iceland’, *Jökull*, 58, pp. 117–138.

Jochum, K. P. *et al.* (2006) ‘MPI-DING reference glasses for in situ microanalysis: New reference values for element concentrations and isotope ratios’, *Geochem. Geophys. Geosyst*, 7, p. 2008. doi: 10.1029/2005GC001060.

Jónasson, K. (2007) ‘Silicic volcanism in Iceland: Composition and distribution within the active volcanic zones’, *Journal of Geodynamics*, 43(1), pp. 101–117. doi: 10.1016/j.jog.2006.09.004.

Koutrouli, A. *et al.* (2018) ‘The early to mid-Holocene marine tephrostratigraphic record in the Nisyros-Yali-Kos volcanic center, SE Aegean Sea’, *Journal of Volcanology and Geothermal Research*. Elsevier B.V., 366, pp. 96–111. doi: 10.1016/j.jvolgeores.2018.10.004.

Lane, C. S. *et al.* (2014) ‘Cryptotephra as a dating and correlation tool in archaeology’, *Journal of Archaeological Science*. Elsevier Ltd, 42(1), pp. 42–50. doi: 10.1016/j.jas.2013.10.033.

Lowe, D. J. (2011) ‘Tephrochronology and its application: A review’, *Quaternary Geochronology*. Elsevier B.V, 6(2), pp. 107–153. doi: 10.1016/j.quageo.2010.08.003.

Lowe, D. J. *et al.* (2017) ‘Correlating tephras and cryptotephras using glass compositional analyses and numerical and statistical methods: Review and evaluation’, *Quaternary Science Reviews*, 175, pp. 1–44. doi: 10.1016/j.quascirev.2017.08.003.

Lowe, J. J. *et al.* (2015) ‘The RESET project: Constructing a European tephra lattice for refined synchronisation of environmental and archaeological events during the last c. 100 ka’, *Quaternary Science Reviews*, 118, pp. 1–17. doi: 10.1016/j.quascirev.2015.04.006.

Martin, E. and Sigmarsson, O. (2007) ‘Crustal thermal state and origin of silicic magma in Iceland: The case of Torfajökull, Ljósufjöll and Snæfellsjökull volcanoes’, *Contributions to Mineralogy and Petrology*, 153(5), pp. 593–605. doi: 10.1007/s00410-006-0165-5.

Matthews, I. P. *et al.* (2015) ‘Developing a robust tephrochronological framework for Late Quaternary marine records in the Southern Adriatic Sea: New data from core station SA03-11’, *Quaternary Science Reviews*, 118, pp. 84–104. doi: 10.1016/j.quascirev.2014.10.009.

Miller, C. F. and Mittlefehldt, D. W. (1982) ‘Depletion of light rare-earth elements in felsic magmas.’, *Geology*, 10(3), pp. 129–133. doi: 10.1130/0091-7613(1982)10<129:DOLREI>2.0.CO;2.

Paterne, M., Guichard, F. and Labeyrie, J. (1988) ‘Explosive activity of the South Italian volcanoes during the past 80,000 years as determined by marine tephrochronology’, *Journal of Volcanology and Geothermal Research*, 34(3–4), pp. 153–172. doi: 10.1016/0377-0273(88)90030-3.

Payne, R. and Gehrels, M. (2010) ‘The formation of tephra layers in peatlands: An experimental approach’, *Catena*. Elsevier B.V., 81(1), pp. 12–23. doi: 10.1016/j.catena.2009.12.001.

Peccerillo, A. (2005) *Plio-Quaternary Volcanism in Italy: Petrology, Geochemistry, Geodynamics*. Springer Berlin Heidelberg New York Library.

Reimer, P. J. *et al.* (2013) ‘Intcal13 and marine13 radiocarbon age calibration curves 0 – 50,000 years cal bp’, 55(4).

Riel-Salvatore, J. and Negrino, F. (2018) ‘Proto-Aurignacian Lithic Technology, Mobility, and Human Niche Construction: A Case Study from Riparo Bombrini, Italy’, in, pp. 163–187. doi: 10.1007/978-3-319-64407-3_8.

Ruffini, R., Cadoppi, P. and D’Atri, A. (1995) ‘Ash layers in the Monferrato (NW Italy) : records of two types of magmatic source in Oligocene-Miocene time Ash layers in the Monferrato (NW Italy): Records of two types of magmatic source in Oligocene-Miocene time’, *Eclogae Geologicae Helvetiae*.

Satow, C. *et al.* (2015) ‘A new contribution to the Late Quaternary tephrostratigraphy of the Mediterranean: Aegean Sea core LC21’, *Quaternary Science Reviews*. Elsevier Ltd, 117, pp. 96–112. doi: 10.1016/j.quascirev.2015.04.005.

Seghedi, I. and Helvac, C. (2016) ‘Early Miocene Kirka-Phrigian Caldera , western Turkey (Eski ş ehir province), preliminary volcanology , age and geochemistry data’, *Journal of Volcan*, 327, pp. 503–519. doi: 10.1016/j.jvolgeores.2016.09.007.

Siebel, W. *et al.* (2011) ‘Acigöl rhyolite field, central Anatolia (part II): Geochemical and isotopic (Sr-Nd-Pb, δ18O) constraints on volcanism involving two high-silica rhyolite suites’, *Contributions to Mineralogy and Petrology*, 162(6), pp. 1233–1247. doi: 10.1007/s00410-011-0651-2.

Smith, E. I. *et al.* (2018) ‘Humans thrived in South Africa through the Toba eruption about 74,000 years ago’, *Nature*, 555(7697), pp. 511–515. doi: 10.1038/nature25967.

Sun, S. -s. and McDonough, W. F. (1989) ‘Chemical and isotopic systematics of oceanic basalts: implications for mantle composition and processes’, *Geological Society, London, Special Publications*, 42(1), pp. 313–345. doi: 10.1144/gsl.sp.1989.042.01.19.

Tomlinson, E. L. *et al.* (2012) ‘The Upper and Lower Nisyros Pumices: Revisions to the Mediterranean tephrostratigraphic record based on micron-beam glass geochemistry’, *Journal of Volcanology and Geothermal Research*, 243–244, pp. 69–80. doi: 10.1016/j.jvolgeores.2012.07.004.

Tomlinson, E. L. *et al.* (2015) ‘The major and trace element glass compositions of the productive Mediterranean volcanic sources: tools for correlating distal tephra layers in and around Europe’. doi: 10.1016/j.quascirev.2014.10.028.

Veres, D. *et al.* (2017) ‘New chronological constraints for Middle Palaeolithic (MIS 6/5-3) cave sequences in Eastern Transylvania, Romania’, *Quaternary International*. doi: 10.1016/j.quaint.2017.07.015.

Vinkler, A. P. *et al.* (2007) ‘Petrology and geochemistry of pumices from the Ciomadul volcano (Eastern Carpathians) -implication for petrogenetic processes’, *Földtani Közlöny*, 137(1), pp. 103–128.

De Vivo, B. *et al.* (2001) ‘New constraints on the pyroclastic eruptive history of the Campanian volcanic Plain (Italy). Mineralogy and Petrology, 73(1-3), 47–65. doi:10.10’, *Mineralogy and Petrology*, 73(1–3), pp. 47–65. doi: 10.1007/s007100170010.

White, W. M. (2013) *Geochemistry*. West Sussex, UK: John Wiley & Sons, Ltd.